Metal-to-metal electron transfer : a powerful tool for the design of switchable coordination compounds

Corine Mathonière

Metal-to-Metal Electron Transfer: A powerful tool for the design of switchable coordination compounds

Corine Mathonière*[a,b]

Dedication to Olivier Kahn

Abstract:
Since the report of photomagnetic effects in Prussian blue Fe/Co networks 20 years ago by the japanese group of Hashimoto, a substantial family of molecular analogs have been obtained and characterized. These compounds offer a unique opportunity to follow metal-to-metal electron transfer by investigating their structural, spectroscopic, electrochemical and magnetic properties. We propose an overview of recent results in order to highlight the common features of these coordination compounds, as well as the differences, with the well-known class of photomagnetic coordination compounds based on spin crossover.

1. Introduction

The field of molecular magnetism emerged at the end of the 1980s. Olivier Kahn, Dante Gatteschi and Roger Willet organized the first meeting of molecular magnetism in 1983 to establish links between chemists, physicists and theoreticians.[1] Indeed, the interdisciplinary aspects in this research field have been one of the keys in the development of molecular magnetism.[2] Speculation about the use of magnetic molecules in modern technology rapidly arose during the 90s.
Olivier Kahn and his coworkers charted the first milestones in this direction of research with the insertion of Fe(II) spin transition compounds in devices.[3] During the same period, Gütlich et al. discovered light-induced excited spin state trapping (the well-known LIESST effect) in $[Fe^{II}(propyl\text{-}tetrazole)_6]^{2+}$.[4] The comprehensive understanding of this phenomenon led to experimental evidence of its reversible character with temperature or light (the reverse LIESST effect).[5] These results opened perspectives for the manipulation of electronic states in coordination compounds with temperature and/or light.
The impact of these results on the scientific community launched the development of a new branch in the field of molecular magnetism devoted to the design and study of switchable coordination compounds. The spin crossover (referred hereafter as SCO) compounds have been the most studied class of switchable compounds, and are the subject of several book series, treating both their chemical and physical properties.[6,7]
In parallel, other switching phenomena at the molecular level have been studied,[8] but in a less extensive manner than the SCO compounds. Amongst them, dioxolene compounds[9] and cyanometallates[10,11] form two other classes of well-studied compounds, where the switching mechanism is based on an electron transfer (named hereafter ET) between the metal ion and one ligand or between two metal ions, respectively.
In this microreview we present the general features of the switching properties in ET compounds through selected examples found in cyanido-bridged FeCo compounds.[12] Several book chapters and reviews have very recently treated these systems, where they were described and sorted by structural and chemical types.[10,13] The purpose of this microreview is different. We do not want to draw an exhaustive panorama of switchable ET compounds but will rather highlight some of their general features. We will first emphasize both the common and the different manifestations of ET processes in selected systems, followed by an examination of the specificity of ET as compared to SCO. We will finish this microreview by presenting several perspectives where ET can be used to generate new effects.

[a] Corine Mathonière
Department of Chemistry, University of Bordeaux
Institute of Chemistry of Condensed Matter in Bordeaux
CNRS, ICMCB, UPR 9048, F-33600 Pessac, France
[b] Univ. Bordeaux, ICMCB, UPR 9048, F-33000 Pessac, France.
E-mail: corine.mathoniere@icmcb.cnrs.fr

Corine Mathonière (born in 1968, France) received her PhD at the University Paris XI under the supervision of Prof. O. Kahn and J.-J. Girerd. After a post-doctoral stay in the group of Prof. P. Day at the Royal Institution of Great Britain in London, she was hired as an associate professor in 1994 at the Université Bordeaux 1 and at the Institut de Chimie de la Matière Condensée de Bordeaux (ICMCB). In 2010, she was promoted professor and obtained a junior member position at the Institut Universitaire de France. She has published around 135 papers and has given more than 65 conferences. Corine Mathonière played a major role in the discovery of the photomagnetic effects in Cu-Mo compounds and has developed a new research area focused on the photomagnetism of electron transfer compounds.

2. Thermally-induced ET: Conversion *vs.* crossover

Generally speaking, SCO and ET generate two isomers that are close in energy and that can be thermally (or optically, see section 3) interconverted. However, the isomerism phenomenon has two different origins: spin isomerism for SCO and valence isomerism for ET. SCO is centered on one single metal ion, and, in line with ligand field theory, complexes with d^4-d^7 electronic configurations may show a thermal equilibrium between low-spin (LS, i.e. strong ligand field) and high-spin

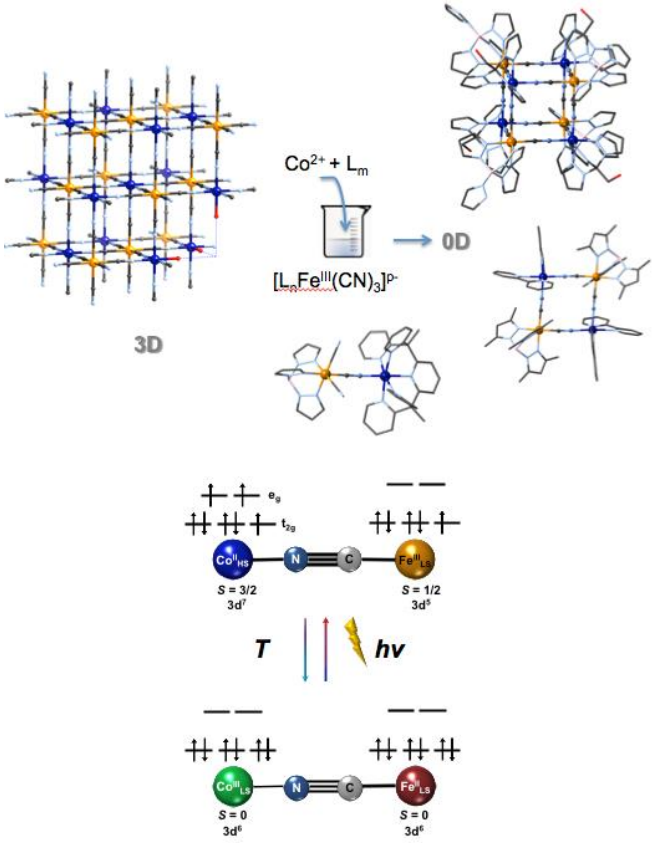

Figure 1 (top) Prussian blue networks (3D, left) and their molecular analogs (right 0D: cube, square and pair. (bottom) Electron transfer (ET) in cyanido-bridged FeCo compounds. The Fe and Co ions in yellow and blue,, respectively**.**

(HS, i.e. weak ligand field) states. ET is the exchange of one electron between two sites, one donor D and one acceptor A, the two valence isomers being the neutral form DA and the ionic form D^+A^-. In this review, we will focus on ET compounds where the D and A units are bridged by a cyanido linker, more specifically on Fe-CN-Co systems.

Figure 1 shows cubic Prussian blue Fe/Co networks[14,15,16] and molecular $[Fe_4Co_4]$ cube,[17] $[Fe_2Co_2]$ square[18] and [FeCo] pair analogs,[19] where metal-to-metal ET has been clearly identified by a variety of characterization measurements. At high temperature, these systems are composed of paramagnetic $Fe(III)_{LS}$-CN-$Co(II)_{HS}$ units. When the temperature decreases, one electron is transferred from the cobalt (donor) to the iron (acceptor) sites to generate the diamagnetic state $Fe(II)_{LS}$-CN-$Co(III)_{LS}$. This ET can be followed by the temperature variation of the infrared spectra, as the CN group is very sensitive to the oxidation state of the bonded metal ions. For instance, the cyanide stretching band in the $Fe(III)_{LS}$-CN-$Co(II)_{HS}$ configuration is located at 2175-2150 cm^{-1}, and is shifted to lower energies (2110-2070 cm^{-1}) in the $Fe(II)_{LS}$-CN-$Co(III)_{LS}$ configuration.[14,15,17,18] Single crystal X-ray diffraction is also a powerful technique to follow electron transfer in these materials. When the temperature decreases, the crystal structures of the molecular analogs show important decreases in Co-N bond lengths, from 2.1 Å to 1.9 Å. This is in agreement with the presence of Co(II) in the high spin configuration (S = 3/2) in the $Fe(III)_{LS}$-CN-$Co(II)_{HS}$ state and in the low spin configuration (S = 0) in the $Fe(II)_{LS}$-CN-$Co(III)_{LS}$ state. This important modification in the Co coordination sphere ($\Delta_{Co\text{-}N}$ ≈ 0.2 Å) between the two valence states is similar to the observed contraction of the Fe^{II}-N bonds in SCO compounds having Fe-N bonds of 2.2 Å in the HS state and 2.0 Å in the LS state. The contraction of the coordination sphere in both cases is explained by the depopulation of antibonding e_g orbitals in the diamagnetic states. Finally, magnetic measurements are particularly useful to follow how ET and SCO proceeds during the temperature variation. These studies give detailed insights about the physics behind the switching processes.

2.1. Electron transfer conversion

Two related squares have been obtained by the reaction of the anionic precursor $[Tp^*Fe(III)CN_3]^-$ (Tp* = tris(3,5-dimethylpyrazolylborate) with Co^{2+} and R-bipyridine in DMF, namely $\{[(Tp^*)Fe^{III}(CN)_3]_2[Co^{II}(Rbpy)_2]_2[OTf]_4\}.n\mathit{Solv}$ with R = Me (**1**) or H (**2**)).[18,20] The Mebpy analog shows a gradual decrease of the χT product (χ being the paramagnetic susceptibility and T the temperature) with decreasing temperature. As often done for SCO compounds, it is convenient to plot the magnetic data as the paramagnetic molar fraction, x, vs. T to directly probe the composition of the system.[2,22] The resulting curve (in red) is presented in Figure 2, and the S-shape is typical of an equilibrium process. This curve may be theoretically reproduced with

$$x_{para} = (1+\exp(\Delta H/R)(1/T - 1/T_{1/2}))^{-1} \qquad \text{Eq. 1}$$

where ΔH is the enthalpy change, T the temperature and $T_{1/2}$ the characteristic temperature of the studied system.

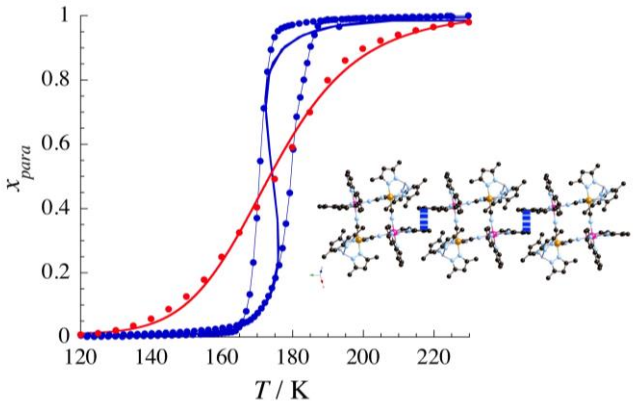

Figure 2 Thermal dependence of the paramagnetic molar fraction x ($x = \chi T/(\chi T)_{300K}$) for two related squares, $\{[(Tp^*)Fe^{III}(CN)_3]_2[Co^{II}(R\text{-}bpy)_2]_4[OTf]_4\}.4DMF.2H_2O$, R = Me (**1**, red curve) and R= H (**2**, blue curve). The thick lines are the fits described in the text, the light one being an eye-guide. Inset: the packing for **2** along a chain showing the close contacts between the squares.

Fitting the experimental data with Eq.1 gives a satisfactory result with the following thermodynamic parameters: the enthalpy change ΔH = 20 kJ mol^{-1} and the temperature $T_{1/2}$ = 174 K, the entropy change being then calculated as $\Delta S = \Delta H / T_{1/2}$ = 115 J K^{-1} mol^{-1}. This means that **1** has a diamagnetic $[Fe(II)_{LS}Co(III)_{LS}]_2$

Table 1. List of the Fe/Co compounds discussed in this review.

Formula [a]	Ref	Dimensionality / Shape	$T_{1/2}$ in K	MMCT λ □□□□□ dia/para	Photomagnetism λ in □□ / thermal stability/ photoinduced magnetism	Compound number
{[(Tp*)$Fe^{III}$$(CN)_3$]$_2$[$Co^{II}$$(Mebpy)_2$]$_2$[OTf]$_2$}.DMF.$H_2O$	20	0D / Square	174	560/770[d]	white / <120 K / para	**1**
{[(Tp*)$Fe^{III}$$(CN)_3$]$_2$[$Co^{II}$$(bpy)_2$]$_2$[OTf]$_2$}.4DMF.$2H_2O$	18a	0D / Square	168/186	525/845[e]	green / < 120 K / para	**2**
{[(Tp*)$Fe^{III}$$(CN)_3$]$_2$[$Co^{II}$$(Mebpy)_2$]$_2$[$PF_6$]$_2$}.CP.BN	24	0D / Square	300/205/195		n.r.	**3**
{[(Tp*)$Fe^{III}$$(CN)_3$]$_2$[$Co^{II}$$(Mebpy)_2$]$_2$[$BF_4$]$_2$}.$H_2$Q. $2H_2O$	25	0D / Square	200	510/700[e]	808 / < 100 K / para	**4**
{[(pzTp)$Fe^{III}$$(CN)_3$]$_4$[$Co^{II}$$(TpOH)_4$]$_4$[$ClO_4$]$_4$}.14DMF.$4H_2O$	17	0D / Cube	250	490/850	white / < 180 K / para	**5**
{[(Tp)$Fe^{III}$$(CN)_3$][$Co^{II}$$(Py5Me_2)$][OTf]}	19b	0D / Pair	167	620	white / < 50 K / para	**6**
{[(pzTp)Fe$(CN)_3$]$_2$[Co(bik)$_2$]$_2$}[ClO_4]$_2$•$2H_2O$	18d	0D / Square	diamagnetic		white / < 100 K / para	**7**
{[(pzTp)Fe$(CN)_3$]$_2$[Co(bik)$_2$]$_2$}[ClO_4]$_2$•$2H_2O$	35	0D / Square	diamagnetic	618	808^{exc} /$532^{de\text{-}exc}$ / para	**7**
K_3{[Fe^{II}(Tp)$(CN)_3$]$_4$[Co^{III}(pzTp)]$_4$[Co^{II}(pzTp)]}	33	0D / Cube	diamagnetic	560 [e]	808 / 100 K / para	**8**
{[(Tp*)$Fe^{III}$$(CN)_3$]$_2$[$Co^{II}$(dtbbpy)$_2$]$_2$[$PF_6$]$_2$}.2MeOH	18c	0D / Square	275/310	560 [e]	808 / 80 K / para	**9**
{[(Tp*)$Fe^{III}$$(CN)_3$]$_2$[$Co^{II}$(dtbbpy)$_2$]$_2$[$PF_6$]$_2$}.2MeOH	36	0D / Square	275/310	770	808^{exc} /$532^{de\text{-}exc}$	**9**
{[(Tp*)$Fe^{III}$$(CN)_3$]$_2$[$Co^{II}$(dtbbpy)$_2$]$_2$[$PF_6$]$_2$} in butyronitrile	18c	0D / Square	227	770/550	n.r.	**9**
{[(Tp*)$Fe^{III}$$(CN)_3$]$_2$[$Co^{II}$(dtbbpy)$_2$]$_2$[$PF_6$]$_2$} in butyronitrile/$H^+$	18c	0D / Square	280	740[e]	n.r.	**9**
{[(Tp*)$Fe^{III}$$(CN)_3$]$_2$[$Co^{II}$(dtbbpy)$_2$]$_2$[$PF_6$]$_2$}.$4H_2O$	18c	0D / Square	diamagnetic	560/770	n. r.	**10**
Na[$_5$(NC)Fe^{II}(CN)Co^{III}(L^{14})]	37	0D / Pair	diamagnetic	510	532 / 8 ps[b]	**11**
Na[$_5$(NC)Fe^{II}(CN)Co^{III}(L^{14S})]	37	0D / Pair	diamagnetic	530	532 / 1.3 ps[b]	**12**
{[Co(tmphen)$_2$]$_3$[Fe$(CN)_6$]$_2$}·xH_2O	39	0D / Pentanucl	> 300	475/670	white / < 75 K / para	**13**
Cs{Co[Fe$(CN)_6$]}	41	3D / PBA NP[c]	diamagnetic	n.r.	650 / few μs[b]	**14**
{[(Tp*)$Fe^{III}$$(CN)_3$][$Co^{II}$(*R*)-pabn][$BF_4$]}.MeOH.$H_2O$	46	1D / Chain	255/280	n.r.	808 / < 75 K / SCM [f]	**15**
{[(pzTp)$Fe^{III}$$(CN)_3$]$_4$[$Co^{II}$(bimpy)][$BF_4$]}.2PrOH.$4H_2O$	47	0D / Hexanucl	220	550/≈900	808 / < 80 K / SMM[f]	**16**
{[(Tp^{Me})Fe$(CN)_3$]$_2$[Co(bpy)$_2$]$_2$[(Tp^{Me})Fe$(CN)_3$]$_2$}·$12H_2O$	50	0D / Square	244	550/≈900	white / < 120 K / para	**17**
[(Tp^{Me})Fe$(CN)_3$]$_2$[[Co(bpy)$_2$]$_2$}·$6CH_3CN$	50	0D / Square	230	n.r.	white / < 120 K / para	**18**
[(BBP)Fe$(CN)_3$Co(PY5Me_2)].$2.5CH_3OH$	51	0D / Pair	228 (SCO Co)	n.r.	n.r.	**19**
{[(Tp*)$Fe^{III}$$(CN)_3$]$_2$[$Co^{II}$(dmbpy)$_2$]$_2$[$PF_6$]$_2$}.$4CH_3CN$	52	0D / Square	paramagnetic	n.r.	not active	**20**
{[(Tp*)$Fe^{III}$$(CN)_3$]$_2$[$Co^{II}$(dmbpy)$_2$]$_2$[$PF_6$]$_2$}	52	0D / Square	230	520	808 / < 100 K / para	**21**
{[(pzTp)$Fe^{III}$$(CN)_3$]$_2$$Co^{II}$(styrylpyridine)$_2$}·$2H_2O$.$2CH_3OH$	68	1D / chain	224/232	n.r.	632/ < 95 K / SCM[f]	**22**
{[(Tp)$Fe^{III}$$(CN)_3$]$_2$$Co^{II}$(Meim)$_4$}·$6H_2O$	73	0D / trinuclear	220/230		532/ < 100 K / para	**23**

[a] Tp* = tris(3,5-dimethyl)pyrazolylborate; Mebpy = 4,4'-dimethyl-2,2'-bipyridine; bpy = bipyridine; pzTp = tetrapyrazolylborate; CP = 4-cyanophenol; BN = benzonitrile, H_2Q = p-hydroquinone; bik = bis(1-methylimidazol-2-yl)ketone; TpOH = tripyrazolylethanol; Py5Me_2 = 2,6-bis(1,1-bis(2-pyridyl)ethyl)pyridine; L^{14} = 6-methyl-1,4,8,11- tetraazacyclotetradecan-6-amine; L^{14S} = 6-methyl-1,4,8,11- tetraazacyclotetradecan-2S-4-amine; tmphen = 3,4,7,8-tetramethyl-1,10-phenanthroline; dtbbpy = 4,4'di-tert-butyl-2,2'-bipyridine; pabn = N(2),N(2')-bis(pyridin-2-ylmethyl)-1,1'-binaphtyl-2,2'-diamine ; bimpy = 2,6-bis(benzimidazol-2-yl)pyridine; Tp^{Me} = hydridotris(3-methylpyrazol-1-yl)borate; BBP = 2,6-bis(benzimidazol-2-yl)pyridine; dmbpy = 5-5' dimethyl-2,2'-bipyridine; Meim = N-methylimidazole. [b] Lifetimes determined by time-resolved spectroscopy. [c] PBA NP = Prussian blue analog nanoparticles. [d] In CH_2Cl_2 at room temperature and at 152 K. [e] PBA NP = Prussian blue analog nanoparticles. [e] In CH_3CN at room temperature and at 160 K. [f] SMM = Single Molecule Magnet. SCM = Single Chain Magnet.

ground state, while the paramagnetic state $[Fe(III)_{LS}Co(II)_{HS}]_2$ is a metastable state populated by the entropy gain. For Fe(II) SCO compounds, the change in entropy values are in the range of 50 to 80 J K^{-1} mol^{-1}.[23] Thus, the large value for the square **1** is surprising at first glance, but if we consider that **1** contains 2 switching Fe/Co units, with each active unit undergoing an entropy change around 57 J K^{-1} mol^{-1}, we see that this is the same order of magnitude as found in mononuclear SCO compounds. It is known that the total entropy is the contribution of electronic and vibrational entropies. The first term can be calculated using statistical thermodynamics ($S = R\ln\Omega$, Ω being the ratio of the total degeneracy in the paramagnetic state over the total degeneracy in the diamagnetic state). Considering one FeCo active unit, the paramagnetic state consists of (i) an LS Fe(III) ion (S = 1/2, $^2T_{2g}$ spectroscopic term in O_h symmetry, leading to the spin and orbital degeneracies of 2 and 3, respectively) and (ii) a HS Co(II) ion (S = 3/2, $^4T_{2g}$, spin and orbital degeneracies being 4, and 3, respectively). The diamagnetic state is a LS Fe(II) (S = 0) and LS Co(III) LS (S = 0) ions both with $^1A_{1g}$ spectroscopic terms for which the spin and orbital degeneracies are 1 and 1, respectively. Finally the total entropy is given by $S = R\ln(\Omega_{para}/\Omega_{dia})$ with Ω_{para}= (2*3)(4*3), and Ω_{dia} = (1*1)(1*1) i.e. $\Omega_{para}/\Omega_{dia}$ = 72, which gives S = 36 J K^{-1} mol^{-1}. This calculation is overestimated because the real Fe and Co site symmetries in **1** are lower than ideal octahedral symmetry, leading to a smaller real electronic entropy. Accordingly, the origin of the remaining entropy in **1** comes from vibrational contributions in the two valence states.

2.2. Electron transfer transition

Now let us consider the magnetic properties of the square **2** with the formula (({[(Tp*)$Fe^{III}$$(CN)_3$]$_2$[$Co^{II}$$(bpy)_2$]$_2$[OTf]$_4$}.4DMF.$2H_2O$). They are plotted on Figure 2 (blue points) for comparison with square **1**. Firstly, the high and low temperatures x values are very similar to those of compound **1**, 1 and 0, respectively. But the thermal variation of the molar fraction x_{para} is now abrupt, and shows a thermal hysteresis of 18 K when the scan rate is fixed at 0.4 K/min. This behaviour is reminiscent of a first order phase transition. For **2**, this interpretation has been confirmed by differential scanning calorimetric (DSC) measurements, showing the presence of enthalpic peaks in cooling and heating modes.[18] Having these DSC data in mind, the magnetic data of

2 can be reproduced with a thermodynamic model where an interaction parameter is added.[22] The results are ΔH = 20 kJ mol^{-1} and the temperature $T_{1/2}$ = 177 K, the interaction parameter Γ = 5.8 kJ/mol and the entropy change being finally calculated as $\Delta S = \Delta H / T_{1/2}$ = 113 J K^{-1} mol^{-1}. Excepting the interaction parameter, all the other thermodynamic parameters are similar for **1** and **2**. This may reflect similar molecular structures in the two compounds, but different intermolecular interactions between the squares. In the two compounds, ET operates with a very different physics. **1** behaves as a collection of switching molecules without interactions between them, and **2** shows a collective switching of the molecules. Similarly to SCO systems, elastic interactions caused by the geometry change around the Co site is probably the origin of cooperativity in **2**. An experimental proof of this hypothesis is obtained by a careful examination of the crystal packing in the two compounds. **2** presents strong π–π interactions between the Co bpy ligands of different squares (see inset in Figure 2), whereas **1** does not show a close packing of the squares, due to the Methyl group on the bpy core. This kind of cooperativity is particularly interesting because it confers to the material a memory effect, which is required for data storage applications.

2.3. Control of the thermally-induced ET

The two squares described in 2.2 are actually textbook cases because the intermolecular interactions are "easy" to recognize in the structures. In other Fe/Co compounds, as for instance in pairs and cubes,[17,19] first-order transitions during the ET are confirmed by thermodynamic and magnetic measurements, but the intermolecular interaction pathways are not clearly identified. Consequently, it remains difficult to predict and control the presence or absence of a thermal hysteresis.

Very recent studies addressed the packing issue by exploiting the directional character of hydrogen bonds. The co-crystallization of a known molecular square {[(Tp*)Fe^{III}(CN)$_3$]$_2$[Co^{II}(Me-bpy)$_2$]$_2$} with hydrogen bonding donors, as 4-cyanophenol in **3**[24] and as p-hydroquinone in **4**,[25] has been realized. The crystal packing of the squares in the two cases are strongly affected by the H bonding between the H donors and the H-acceptors (the remaining available CN groups). The compound with the cyanophenol donor **3** presents a three-step electron transfer (Figure 3) revealing four states: the HT and the LT phases described above, and two additional intermediate phases (IM1 and IM2). With the help of X-ray structural studies, this peculiar behavior was associated with a phase transition, causing a symmetry breaking and a doubling of the unit cell. In the IM1 and IM2 phases, the presence of crystallographically distinct squares, accompanied by an alteration of H bonding, allows the assignment of the different plateaus observed in Figure 3. Moreover, when cyanophenol is removed in the dried compound, the ET disappears, confirming the role of the cyanophenol in the observed behaviour. These results suggest that multistability can be driven by a dynamic control of solid-state hydrogen bonds. This finding opens a new route for chemists to design new switchable materials.

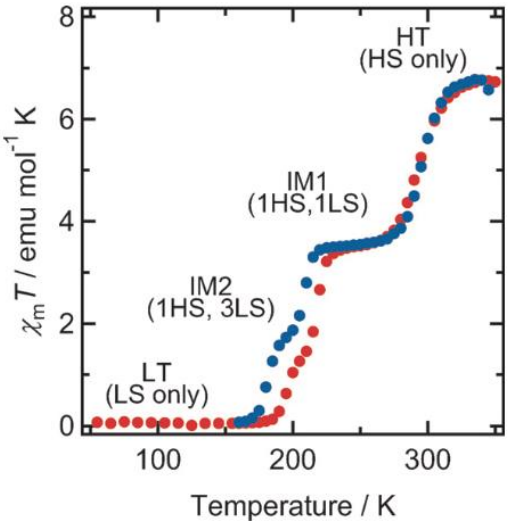

Figure 3: χT vs. temperature plot for the square {[(Tp*)Fe^{III}(CN)$_3$]$_2$[Co^{II}(Mebpy)$_2$]$_2$[PF$_6$]$_2$}.CP.BN, **3**, cooling (blue) and heating (red). Reproduced with permission from ref. 24.

3. Light-induced ET

The LIESST (Light Induced Excited Spin State Trapping) effect in [[Fe^{II}(propyl-tetrazole)$_6$](BF$_4$)$_2$, was discovered several decades after the first evidence of a thermally-induced spin transition, reported by Cambi et al.[26] This discovery opened a new research direction in molecular magnetism devoted to photomagnetic materials.[27] Today, many spin crossover compounds are known to exhibit thermal and photo-induced SCO in different temperature ranges. In the course of the discovery of new photomagnetic effects, the photo-induced ET modification of the magnetic properties in the 3D Prussian blue analog, $K_{0.2}Co_{1.4}[Fe(CN)_6]$. 6.9$H_2O$ from an "almost" diamagnetic state to a ferrrimagnetic state,[14,15] also had a strong impact in this research field. For the first time, a huge increase of the magnetization was obtained by light, even at low magnetic field. $K_{0.2}Co_{1.4}[Fe(CN)_6]$. 6.9$H_2O$ was declared as the first photomagnet in the Prussian blue analogs. But, at that time, this photo-induced ET was not associated with any thermally-induced ET, as described in the previous section. This phenomenon was discovered later, in 2001, by Bleuzen et al. in related Prussian blue $C_xCo_x[Fe(CN)_6]_y$ (C = K or Cs$^+$) analogs.[28] The similarities with the SCO phenomenon became more and more obvious with the presence, in both cases, of two states, one being the ground state and the second being a metastable state. For both processes, the metastable states can be populated with an increase of temperature or by light irradiation at low temperature. These transformations are fully reversible for SCO and ET processes.

3.1. Photomagnetism in molecular analogs

After the discovery of photomagnetic Prussian blue analogs, the further development of ET systems, in particular with the generation of a large family of complexes using the building

block approach and heteroleptic complexes, definitively confirmed the similarities between SCO and ET. A nice example of this is shown by the magnetic properties of the $[Fe_4Co_4]$ cube, $\{[(pzTp)Fe^{III}(CN)_3]_4[Co^{II}(TpOH)_4]_4[ClO_4]_4\}.14DMF.4H_2O$, **5**, the first isolated cubic fragment of a Co/Fe Prussian blue analog. The magnetic properties of the cube are shown in Figure 4, measured in different temperature and/or light conditions.[17] In the dark, **5** shows a χT value of 12.7 cm^3 K mol^{-1} at room temperature, in agreement with four Fe(III) ions in the low spin state and four Co(II) ions in the high spin state. When the temperature is decreased, an abrupt transition occurs with $T_{1/2}$ = 250 K. The compound is diamagnetic below 220 K, consisting of a $[Fe(II)_4Co(III)_4]$ cube, as a result of a metal-to-metal electron transfer. At 30 K, when **5** is submitted to white light irradiation, a progressive increase of the χT value is observed, reaching a value of 10 cm^3 K mol^{-1} after 20 hours. The light-induced paramagnetic $[Fe(III)_4Co(II)_4]$ state then relaxes to the diamagnetic state when **5** is heated again in the dark at 180 K. Moreover, the metastable state can be also generated by rapid cooling, as shown in Figure 4.

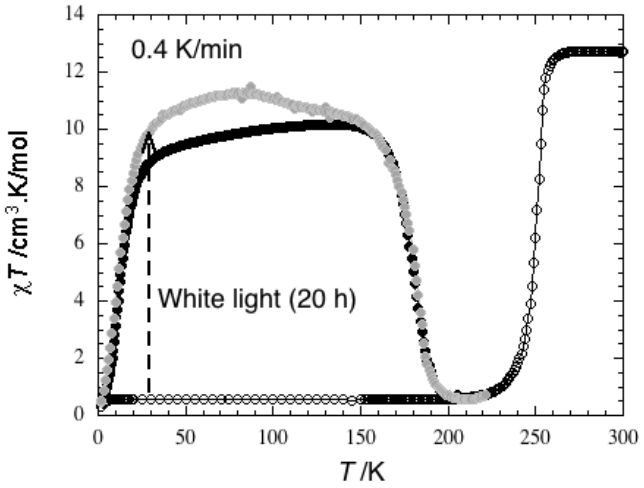

Figure 4: χT versus temperature plots for the cube, $\{[(pzTp)Fe^{III}(CN)_3]_4[Co^{II}(TpOH)_4]_4[ClO_4]_4\}.14DMF.4H_2O$, **5**, before irradiation (white circles), after irradiation (gray circles), and after thermal quenching (black circles).

These types of magnetic curves, showing a thermally-induced ET at high temperature in cooling/heating modes and a light-induced effect at low temperature, have been well described for SCO compounds.[27,29] Additionally, SCO and ET mechanisms generate concomitant changes of magnetic and optical properties, which lead to photomagnetic and photochromic properties. These aspects are very important for applications because the optical properties can be used for devices and sensors.

Generally, photomagnetic SCO compounds present the LIESST effect below a temperature in the range 50 K - 70 K. This temperature range is significantly larger (up to 110 K) for some particular cases when the SCO is associated with the formation of an seventh Fe-N bond, such as in $[Fe(LX_5)(CN)_2].H_2O$ complexes, with LX_5 being a macrocyclic ligand.[30] In the ET systems, photomagnetic effects up to 50 K have been reported in the [FeCo] pair **6**,[19] and up to 100-120 K for the majority of the squares (see Table 1).[12,18] This temperature range is significantly increased up to 180 K for the $[Fe_4Co_4]$ cube **5**.[17] This is the highest temperature reported so far for switchable coordination compounds. It is worthwhile to note that a direct comparison of these temperatures for the different compounds is not strictly possible, as they are dependent on the scan rates used during the temperature increase, which are not always mentioned in the reported studies.

The precise estimation of the lifetimes of the metastable states requires time dependence studies of the susceptibilities at different temperatures. These measurements track the relaxation of the metastable states and allow the extraction of the relaxation time τ(T). Plotting τ versus 1/T leads to the determination of the activation energy using the Arrhenius law ($\tau = \tau_0 \exp(-\Delta/k_BT)$). Studying the population of the light-induced states (over several hours) and the relaxation processes is very time-consuming. Consequently, such studies have been realized for only few ET compounds, namely the square **2** and the cube **5** (Table 1).[17,18] The energy gap between the diamagnetic ground state and the metastable state has been estimated at 2854 K with $\tau_0 = 9.1\ 10^{-9}$ s for **2**, and at 4455 K with $\tau_0 = 2.6\ 10^{-8}$ s for **5**. The higher value of the energy gap for **5** is in perfect agreement with the larger temperature range for the stability of the photo-induced state. The lifetime at 120 K of this metastable state has been calculated using the parameters deduced by relaxation studies, and has been estimated at 10 years. For comparison, similar studies have been done for Fe/Co Prussian Blue networks, $Na_{0.4}Co_{1.4}[Fe(CN)_6].3.4H_2O$ and gave rise to the following paramaters $\tau_0 = 6.7\ 10^{-7}$ and 3110 K, or a corresponding lifetime at 33 hours at 120 K.[31]

Even if the $[Fe_4Co_4]$ cube currently possesses the highest lifetimes amongst Fe/Co systems, it does not hold the record for switchable coordination compounds. An SCO trimer of Fe(II) ions, namely $[Fe_3(\mu\text{-}L)_6(H_2O)_6]$ with L = 4-(1,2,4-triazol-4-yl)ethanedisulfonate, exhibits a relaxation temperature of 250 K for the thermally quenched state.[32] But, on the whole, the photoactivity of the ET Fe/Co compounds presents two interesting features: (i) the lifetimes of the photo-induced states are significantly higher than in other photomagnetic compounds, and (ii) it can be controlled by the stoichiometry of the systems, increasing with the number of pairs in the compounds. This last characteristics seem quite general. For instance, the compound **7** consists at room temperature of $[Fe(II)_2Co(III)_2]$ squares, and is therefore diamagnetic. An ET spontaneously occurs during its synthesis between the Fe(III) and the Co(II) ions present in the starting materials. Even if this compound is not showing a thermally-induced ET, it presents a paramagnetic photo-induced state with a relaxation around 100 K, temperature in agreement with the square structure of the compound. In Table 1, a new $[Fe_4Co_4]$ cube, $K_3\{[Fe^{II}(Tp)(CN)_3]_4[Co^{III}(pzTp)]_3[Co^{II}(pzTp)]\}$ **8**, has been isolated with potassium located inside the box.[32] The cube is diamagnetic up to 300 K and is photomagnetic below 100 K, i.e. far from the 180 K measured for the $[Fe_4Co_4]$ box **5**. At the first glance, the photo-induced ET behaviour in the box **8** seems in contradiction with the previous statement tending to show a relation between stoechiometry and relaxation

temperature. But actually as **8** contains only three active $Fe^{III}Co^{II}$ pairs, it can not be considered as a "photomagnetic" cube. This can be an explanation of the discrepancy of the relaxation temeprature between **5** and **8**.

Photoreversibilty is an another important issue for photo-switchable compounds. If the two energies of the probed states during photo-excitation are sufficiently well-separated in energy, optical population and its reverse effect (optical depopulation) can be realized. The resulting photoreversibilty (or reversible optical switching) is important and can be used for applications in optical data storage. It is worth noting that the first report of the photomagnetic effect in Fe/Co Prussian blue analogs[14] mentioned a red-light excitation from the diamagnetic to ferrimagnetic states, as well as the back ET trasnformation using blue light.

As shown in Table 1, the population of the $\{Fe^{III}Co^{II}\}$ paramagnetic state from the $\{Fe^{II}Co^{III}\}$ diamagnetic state can be achieved with a large variety of excitation wavelengths, with white light, or even with X-ray irradiation for the square **9**.[34] In the optical spectra of these species, the MMCT band (Fe^{II} ➔ Co^{III}) is usually located in the 500-800 nm range. Several studies investigated the w□□□□□□□□□ dependence of the excitations. Using surface optical reflectivity techniques, the pair **6** was found to be excitable with wavelengths ranging from 1050 to 360 nm. Nevertheless, the best efficiency for photoexcitation is obtained in the NIR region, in agreement with the position of the MMCT band.[19] Only one study has demonstrated the photoreversibility by following the ET process by magnetic and structural measurements.[35] Figure 5 shows the effect of four successive irradiations of the square **7**, such that a 808 nm excitation at 20 K led to an increase in the χT product, in agreement with the population of the paramagnetic state, while

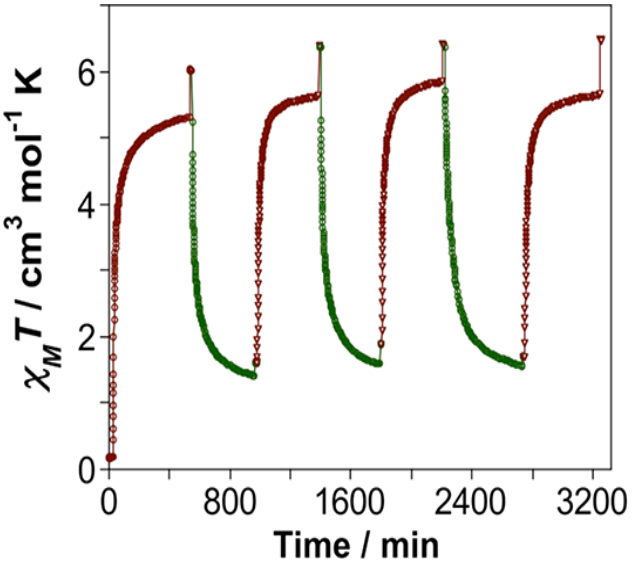

Figure 5: Plot of $\chi_M T$ vs time for the square $\{[(pzTp)Fe(CN)_3]_2[Co(bik)_2]_2\}$-$[ClO_4]_2 \cdot 2H_2O$ **7** under cycles of successive irradiation at 808 nm (6 mW/cm^2) and 532 (10 mW/cm^2) nm at 20 K. Reproduced with permission from ref. 35.

a further 532 nm excitation results in the opposite variation of the χT product. This decrease has been interpreted as a partial light-induced depopulation of the paramagnetic state, as the χT product remains stable at 20 K when the first excitation at 808 nm is stopped, and starts to decrease only when the second excitation at 532 nm is launched. There is another study showing a second case of a similar partial photoreversible ET in the square **9**.[36] The photoreversibility is again partial, maybe because an overlap exists between the 2 MMCT bands (Fe^{II} ➔ Co^{III} and Co^{II} ➔ Fe^{III}, for the diamagnetic and paramagnetic states, respectively).

3.2. Mechanism of photo-induced ET

To describe the properties of these Fe/Co ET systems, several acronyms have been used. ET refers to the general process, and describes only the initial and final products. But considering the spins associated with the metal ions, one of these states is the diamagnetic $(Fe(II)_{LS,S=0}\text{-}CN\text{-}Co(III)_{LS,S=0})$ state, whereas the second is a paramagnetic $(Fe(III)_{LS,\,S=1/2}\text{-}CN\text{-}Co(II)_{HS,\,S=3/2})$ state. In fact, this simple description corresponds to a spin forbidden process. Therefore, it is necessary to insert intermediate states to explain the efficiency of the process, i.e. through pathways involving spin-allowed transitions.

To elucidate the intimate mechanism of the ET, transient absorption spectroscopies are a good tool to detect intermediate states. But few studies of this type have been reported for ET compounds. One study concerns the [FeCo] pairs $Na[_5(NC)Fe^{II}(CN)Co^{III}(L^{14})]$ and $Na[_5(NC)Fe^{II}(CN)Co^{III}(L^{14S})]$, **11** and **12**.[37] The second study examines the Fe/Co Prussian blue analog, $Na_{0.35}Co[Fe(CN)_6]_{0.79}.3.7H_2O$.[38] Both works established the existence of a short-lived intermediate state that slowly relaxes towards the long-lived photo-induced state. It has been proposed that the intermediate state is characterized by an $Fe(III)_{LS,\,S=1/2}\text{-}CN\text{-}Co(II)_{LS,\,S=1/2}$ moiety. This interpretation means that the initial electron transfer between the two metal ions is followed almost immediately by a spin crossover on the Co ions.

The term Charge Transfer Induced Spin Transition (abbreviated as CTIST) was used for the first time in 2002 by the Hashimoto group.[15d] Later the Dunbar group used it to describe the ET phenomenon obtained in the first cyanido-bridged Fe/Co compounds, $\{[Co(tmphen)_2]_3[Fe(CN)_6]_2\}\cdot xH_2O$, **13**, formed by a trigonal bipyramidal Fe_2Co_3 core geometry.[39] Even if this CTIST acronym was introduced before the publication of ultrafast spectroscopy results, it is actually in agreement with the more recent experimental conclusions.[37,38] Another acronym, ETCTS[40] for Electron-Transfer-Coupled Spin Transition, was used by the Oshio group to describe ET in similar Fe/Co systems. This acronym is more precise in describing the charge delocalization, as one electron (and not a partial charge), is fully transferred with decreasing temperature or under light irradiation. ETCTS is also in agreement with magnetic and structural experimental results pertaining to the two states. But the ETCTS description is also more conservative about the different steps during the ET, as it does not define which event, the electron transfer or the spin crossover, triggers the other one.

To experimentally identify the valence states of the metal ions in the intermediate states without ambiguity, transient X-ray absorption spectroscopy (XAS) has been recently used for nanoparticles of the 3D network Cs{Co[Fe(CN)$_6$]} **14.** The transient spectra at the Fe and Co K-edges have been measured and show that is it possible to follow ET by time-resolved XANES (X-ray Absorption Near Edge Spectroscopy), at the two edges at room temperature.[41] The ET process occurs at the picosecond timescale and the lifetime of the intermediate state can be probed further by femto-second optical spectroscopy is comprised in the 1-10 μs range. In the future, these time-resolved XAS experiments, performed with a better time resolution (at the fs timescale), will bring some important insights about the intermediate states during the ET process.

3.3 Photo-induced paramagnetic state: Ferromagnetic or antiferromagnetic interactions?

The CN ligand plays an important role in molecular magnetism, because it is known as a good coordination linker due to the simultaneous presence of lone pairs on the C and N atoms. As an example, the Prussian blues and their analogs have been known by coordination chemists for a long time.[42] Moreover, this linker is an efficient transmitter of the exchange interaction, because of the triple-bond character of the CN bond. Actually, the reputation of "CN" in molecular magnetism increased a great deal when the first room-temperature molecule-based magnet in the 3D network, $V^{II}[Cr^{III}(CN)_6]_{0.86}.2.8H_2O$ was reported.[43] It should be mentioned that magnetic Prussian Blue analogs have been particularly well studied by the teams of Verdaguer and Girolami. For example, the 3D network $Co_{1.5}[Fe(CN)_6].6H_2O$ shows a ferromagnetic ordering below 16 K in its ground state, (although this compound is not ET active and remains in its $Co^{II}_{1.5}Fe^{III}$ state at all temperatures).[44] Later, the photo-induced state in $Rb_{1.8}Co_4[Fe(CN)_6]_{3.3}.13H_2O$ was studied with X-ray Magnetic Circular Dichroism (XMCD). This technique is able to measure the local magnetizations at the Fe and Co K-edges and their relative orientations with an external magnetic field. The results of this study provide the first local experimental proof of the antiparallel orientation of the Fe(III) and Co(II) ions in the photomagnetic 3D network.[45]

Concerning the molecular analogs, magnetic studies of the photo-induced states of squares, pairs and cubes show increases[18a,d] or decreases[20,24,25,17,19b,33] of the χT product when the temperature decreases in the low temperature region (i.e. well below the thermal relaxation of the photo-induced states). These behaviors suggest respectively intramolecular ferromagnetic or antiferromagnetic interactions between Co^{II} and Fe^{III} ions. Moreover, some other compounds composed of 1D chains, namely {[(Tp*)$Fe^{III}(CN)_3$][Co^{II}(*R*)-pabn][BF_4]}.MeOH.H_2O **15**,[46] and a square decorated with two Fe(III) arms, namely {[(pzTp)$Fe^{III}(CN)_3]_4[Co^{II}$(bimpy)]$_2$[$BF_4$]}.2PrOH.4$H_2O$ **16**,[47] clearly show a net increase of the χT product when the temperature decreases. This can be only attributed to ferromagnetic interactions. In these cases, magnetic correlation along the chain in **15** and the large quantity of paramagnetic ions in **16** helps the experimental verification of the ferromagnetic nature of the intramolecular exchange interaction. In the other systems mentioned above, the weakness of these interactions can be easily hidden by strong spin-orbit coupling in both the low-spin Fe(III) and Co(II) ions. Nonetheless, calculations on some paramagnetic Fe/Co squares, theoretically demonstrated the presence of intramolecular ferromagnetic interactions.[48] Clearly, the exchange interactions in these systems are far from being fully understood. Further investigations are necessary to elucidate the nature of the exchange interactions between the Fe and Co ions. In particular, the use of XMCD techniques for the molecular analogs will be a good choice to bring more information about the exchange interactions.

4. Chemical design of ET systems.

This section is devoted to the chemical tools for the design of new ET Fe/Co species with controlled properties. The primary idea developed by molecular chemists was to control the growth of the species step-by-step. This so-called building-block approach has been used with great success for the isolation of molecular analogs of magnetic and photomagnetic Prussian blue analogs.[18c] This strategy is based on the use of bulky ligands around the metal centers to allow only limited sites in the desired directions to coordinate via the CN groups. While this approach can be considered as an appealing structural strategy, it neglects the influence of the electronic effects of the different components. The first experimental evidence of ET in the molecular box **5** was obtained by chance, neglecting any electronic control of the ET. But after the advent of the first molecular analogs, the possibility of tuning of the electronic properties of the different components has received greater interest. Considering the Marcus and Hush theory of electron transfer reactions,[49] it is of crucial importance to consider the redox potential difference between the partners as an important parameter to control the ET.

4.1. ET as an internal redox process

Several studies have used the redox potential difference in the constituent metallic moieties as an experimental factor to understand the properties of the final compounds. The first report of electrochemical studies of ET squares appeared in 2010.[18c] In this work, the authors described the cyclic voltammetry (CV) of three squares in CH_3CN at room temperature, **9**, **10** and {[(Tp)$Fe^{III}(CN)_3]_2[Co^{II}$(dtbbpy)$_2]_2$[$PF_6$]$_2$}.4$H_2O$. They evaluated for each compound the redox potential difference, $\Delta E = E_{Co(III)/Co(II)} - E_{Fe(III)/Fe(II)}$, from the CV in CH_3CN. They concluded that the value of ΔE determined as 0.41 V allows the observation of thermally-induced ET in **9**. A second study using electrochemistry as a guide to tune the ET behavior in squares was reported by Holmes et al. in 2014.[50] In this work, a new Fe(III) building block, $[(Tp^*)Fe(CN)_3]^-$, was prepared by slightly modifying the complex used for the preparation of the original square. Tp* is a

substituted Tp ligand having two donor Me groups grafted on its pyrazole moieties, and the new ligand Tp^{Me}, with only one Me on each pyrazole moiety, furthermore allowed the formation of the new building block $[(Tp^{*})Fe(CN)_3]^{-}$. The removal of one methyl group to give the Tp^{Me} ligand decreases the electronic density on the Fe site, as confirmed by electrochemical studies for this new complex. Moreover, this effect has been rationalized in the same paper by a detailed CV study of the known $[(Tp^{R})Fe(CN)_3]^{-}$ complexes. The more donor groups the ligand contains, the lower the redox potential. Therefore the Fe(II) site is stabilized. The two new squares **17** and **18** obtained with this new precursor display $T_{1/2}$ at 244 and 230 K, respectively, well above the $T_{1/2}$ at of 177 K found in the original square **2**.[50] This result shows that the modulation of the thermal-induced ET can be easily controlled by electronic effects of the ligands borne by the metal ions.

The redox properties have been also used for the design of [FeCo] pairs. The first pair obtained in the family of Prussian blue molecular analogs, $[(BBP)Fe(CN)_3Co(PY5Me_2)].2.5CH_3OH$ **19**, was designed considering the steric hindrance of the ligands around the Fe and Co sites.[51] For the Fe ligand, the tridente ligand, BBP^{2-} (the deprotonated form of 2,6-bis(benzimidazol-2-yl)pyridine) has been chosen, competed by three coordinating CN groups arranged in a meridional geometry. The driving force for the formation of the pair is brought by the pentadente ligand $PY5Me_2$ around the Co, for which only one remaining position is available for the formation of a CN bridge with the Fe ion. Surprisingly, the obtained compound **19**, does not show an ET process, but rather a SCO on the Co(II) metal ion with a $T_{1/2}$ of 228 K (Table 1), as confirmed by the crystal structures measured at 370 and 90 K. This compound has been further studied in solution, and in particular the effect of ligand protonation on its ET properties. Nihei et al. have shown that the protonation of the square **9** in butyronitrile solution can modulate the thermal-induced ET with an increase of the $T_{1/2}$ from 227 K to 280 K.[18c] The authors interpreted this shift as the protonation

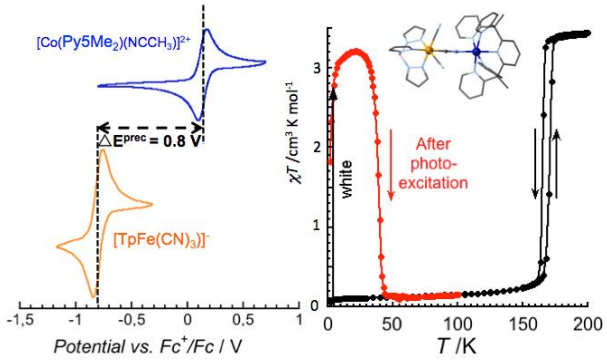

Figure 6 (left) Cyclic voltammetry of the two precursors $[Co(Py5Me2)]^{2+}$ and $[TpFeCN_3]^{-}$ used for the synthesis of the pair **6** (right) Plot of χT vs temperature for the pair $\{[(Tp)Fe(CN)_3][Co(Py5Me_2](OTf)\}$ **6** in the dark (black points, 0.4 K/min)) and after white light irradiation at 10 K.

of the free CN around the Fe site, which decreases the electronic density around the Fe and consequently favors the diamagnetic square. Following these results, the protonated pair $[(H_2BBP)Fe(CN)_3Co(PY5Me_2)]$ was formed in solution, and studied by electrochemical, UV-vis and NMR techniques. The result was a strong positive shift of the redox potential of the $[(H_2BBP)Fe(CN)_3]$ complex, which was then crystallized, revealing the protonation of an N atom belonging to the pyrazole unit of the ligand. This shift explains the diamagnetic nature of the protonated $[(H_2BBP)Fe^{II}(CN)_3Co^{III}(PY5Me_2)]$ pair. The study of **19** and its protonated version **$H_2$19** inspired the conception of a building block strategy based on the redox potentials of the Fe and Co precursors. To illustrate this idea, it seems likely that **19** is paramagnetic because the redox potential difference of the two building blocks is too large ($\Delta E_{precursors}$ = 1.1 V), while the **$H_2$19** compound is diamagnetic because $\Delta E_{precursors}$ is too small (0.46 V). From the vast library of $[LFeCN_3]^{-}$ complexes, $[TpFe(CN)_3]^{-}$ has been selected as an appropriate building block to react with the $[Co(Py5Me_2)]^{2+}$($\Delta E_{precursors}$ = 0.8 V).This strategy has been successfully used to elaborate the first isolated [FeCo] pair displaying thermal- and light-induced ET (figure 6).[51]

The tuning of thermal-induced ET is a very attractive opportunity when working in solution. But the examples cited in the previous paragraphs hide a very difficult problem that arises when the compounds are crystallized. For example, the same molecular square $\{[(Tp^{*})Fe^{III}(CN)_3]_2[Co^{II}(Mebpy)_2]_2]\}^{2+}$ contained in **1**, **3** and **4**, shows different thermal-induced ET behaviors in solid state depending on the compensating anions and/or the solvents of crystallization (see Table 1). The molecular packing of the squares in **3** and **4** display an H-bonding network involving the Fe-CN units as acceptors. The increase of $T_{1/2}$ has been again interpreted as an increase of the redox potential of the Fe site and the better stability of the diamagnetic squares. The role played by anions and/or co-crystallized solvents is difficult to predict in advance, and can undermine all strategies based on redox potentials measured in solutions. A nice illustration of that is the example of the squares **20** and **21**.[52] The solvated form of **20** is paramagnetic whereas the dried version **21** is ET active with a thermally-induced and light-induced ET. A more recent example is given by the trigonal bipyramidal compound $(Et_4N)[\{Co(L)_2\}_3\{Fe(CN)_6\}_2](ClO_4)\cdot 13EtOH$, L being *N*-2-pyridylmethylene-(S)-(+)-1,2,3,4-tetrahydro-1-naphthylamine, that shows a thermally-induced ET by solvent desorption and re-absorption.[53]

Finally, a means of circumventing the uncertainties generated by the crystal packing is to tune the ET in solutions. Two squares 1 and 9 have been solubilized in different media to create thermochromic solutions.[20,18c] For 1, solvents of different polarities and/or different compositions have been studied. The ET has been followed by the temperature dependence of the UV-Vis spectra and magnetic studies in solutions. The results indicated that increasing solvent polarity results in an increase

Table 2. List of the cyanido-bridged M/M' compounds discussed in this review.

Formula [a]	Ref	Dimensionality / Shape	$T_{1/2}$ / K	Valence isomers	Photomagnetism λ (□□) / thermal stability / Photo-induced magnetic phase
$Rb_xMn_y[FeCN_6].nH_2O$	55	3D / PBA[b]	225/300	$Mn^{II}Fe^{III}/Mn^{III}Fe^{II}$	532/ n.r. / AF T_N = 17 K
$A_xFe_y[Cr(CN)_6].nH_2O$	56	3D / PBA	none	$Fe^{II}Cr^{III}/Fe^{III}Cr^{II}$	blue / n.r.
$Co_3[Os(CN)_6]_2{\cdot}6H_2O$	57	3D / PBA	245	$Co^{II}Os^{III}/Co^{III}Os^{II}$	white / < 165 K / FI T_c = 17 K
$Cs[\{Co(3\text{-cyanopyridine})_2\}]\{W(CN)_8\}.H_2O$	58	2D	167/216	$Co^{II}W^{V}/Co^{III}W^{IV}$	red / < 120 K/ F T_c = 30 K
$Co_3[W(CN)_8]_2(pyrimidine)_4{\cdot}6H_2O$	59	3D	298/208	$Co^{II}W^{V}/Co^{III}W^{IV}$	532 / < 150 K / F T_c = 40 K
$[Co^{II}(bik)_3][\{W(CN)_8\}_3\{Co(bik)_2\}_3]{\cdot}2H_2O{\cdot}13CH_3CN$	60	0D / hexanuclear	215	$Co^{II}W^{V}/Co^{III}W^{IV}$	808 / < 120 K / para
$\{Co_3Fe_6[W(CN)_8]_6(MeOH)_{24}\}.xMeOH$	61	0D / pentadecanuclear	194/207	$Co^{II}W^{V}/Co^{III}W^{IV}$ +$Fe^{II}W^{V}/Fe^{III}W^{IV}$	n.r.
$\{[Fe(tmphen)_2]_3[Os(CN)_6]_2\}$	62	0D / pentanuclear	200-350	$Fe^{II}Os^{III}/Fe^{III}Os^{II}$	n.r.
$Cu_2[Mo(CN)_8].2H_2O$	63a	3D	none	$Cu^{I}Mo^{V}/Cu^{II}Mo^{IV}$	405 / < 180 K / FI T_c = 13 K
$CsCu_{1.5}[Mo(CN)_8].2H_2O$	63b	3D	none	$Cu^{I}Mo^{V}/Cu^{II}Mo^{IV}$	405 / < 180 K / FI T_c = 23 K
$\{[Cu(tren)]_6[Mo(CN)_8](ClO_4)_8\}$	64	0D / heptanuclear	none	$Cu^{I}Mo^{V}/Cu^{II}Mo^{IV}$	405 / < 280 K / paramagnetic

[a] bik = bis(1-methylimidazol-2-yl)ketone]; tmphen = 3,4,7,8-tetramethyl-1,10-phenanthroline. tren : triethylene-diamine. [b] PBA = Prussian blue analogs.

in the ET temperature. For instance, the $T_{1/2}$ shifts from 180 K in CH_2Cl_2 to 240 K in CH_3OH.

4.2 Extension to other systems

The SCO process is usually limited to 3d metal ions having an d^4-d^7 electronic configuration. ET is more general as the switching process can happen for other metal ion pairs, as long as the donor and acceptor units are linked by an adequate bridge. For example, in cyanide-bridged systems, several pairs are known to present thermally-induced and light-induced ET. Similarly to the Fe/Co networks, the first evidence of ET for other couples has been achieved in cyanido-bridged networks (Table 2).[54] For example, the Prussian blue analogs, $Rb_xMn_y[FeCN_6].nH_2O$[55] $A_xFe_y[Cr(CN)_6].nH_2O$[56] and $Co_{1.5}[OsCN_6].3H_2O$,[57] show thermal- and light-induced properties due to a metal-to-metal ET. If the Co/Os Prussian blue analog is behaving as a photomagnet with a ferrimagnetic ordering, the Mn/Fe analog has a photo-induced antiferromagnetic phase. Other related photomagnetic networks have been synthetized from the octacyanido $[M(CN)_8]^{4-}$ precursors. The 2D $Cs[\{Co(3\text{-cyanopyridine})_2\}]\{W(CN)_8\}.H_2O$[58] and the 3D $Co_3[W(CN)_8]_2(pyrimidine)_4{\cdot}6H_2O$[59] networks reported by the Ohkoshi group present photo-induced ferromagnetic ordering, due to ET between Co and W between metal centers. After the demonstration of the remarkable ET properties of these new networks, molecular analogs were isolated following similar chemical strategies to the ones used for Fe/Co molecules. But up to now, they are limited to only few examples. For the Co/W(CN)$_8$ couple, the two reported compounds (Table 2) have original structures. $[Co(bik)_3][\{W(CN)_8\}_3\{Co(bik)_2\}_3]{\cdot}2H_2O{\cdot}13CH_3CN$[60] is made of a $[Co_2W_2]$ square with a $Co^{III}W^{V}$ tail and a counter ion $[Co^{II}(bik)_3]^{2+}$. The ET in this compound occurs in the square between the diamagnetic $[Co^{III}_2W^{IV}_2]$ and paramagnetic $[Co^{II}_2W^{V}_2]$ states. $\{Co^{II}_3Fe^{II}_6[W^{V}(CN)_8]_6(MeOH)_{24}\}.xMeOH$ is a trimetallic nanosized cage that shows thermally-induced ET between Co and W metal ions, but also between Fe and W ions as confirmed by Mossbauer studies.[61] Unfortunately, this interesting compound has not been studied under light irradiation, because it looses easily its morphology because of solvent loss. Another photomagnetic molecule with the formula $\{[Fe^{II}(tmphen)_2]_3[Os^{III}(CN)_6]_2\}$ has been described having the same structure than the trigonal bipyramidal compound **13**, ie. $\{[Co(tmphen)_2]_3[Fe(CN)_6]_2\}$.[62] This compound is the first and unique example of thermally-induced ET between Fe and Os metal ions.

It is important to note here that other photomagnetic molecule-based systems obtained within the couple Cu/Mo(CN)$_8$, described as 3D networks[63] or finite molecules,[64] are known in the literature (Table 2). The first photomagnetic studies of these compounds mentioned an ET process between Cu^{II} and Mo^{IV} ions to explain the observed properties. But theoretical and experimental recent studies proposed an alternative spin crossover on the Mo^{IV} ion to explain the observed behaviours.[65] To solve this question, several groups prepared a significant number of Cu/Mo(CN)$_8$ compounds with different stoichiometries.[66] But up to now, the mechanism is still under debate for the Cu/ Mo(CN)$_8$ couple.

5. Other external perturbations to induce ET: Towards multifonctional compounds

In some compounds, ET has been used to generate not only thermal- and light-induced properties but also interesting magnetic features, such as Single-Molecule Magnetic behaviour (SMM.)[67] The SMM properties are interesting because they offer magnetic bistability, ie. the manipulation of two distinct magnetic states + M and -M. The first example of photo-induced SMM was given by the hexanuclear compound **15** which can be described as a Fe/Co square bearing two additional $[pzTpFe(CN)_3]^-$ units linked to the internal $[Fe_2Co_2]$ square. The thermally-induced ET in **15** was followed by Mössbauer and magnetic measurements, which indicated a change from the HT $[Fe^{III}_{LS}(Co^{II}_{HS2}Fe^{III}_{LS2})Fe^{III}_{LS}]$ state to the LT $[Fe^{III}_{LS}(Co^{III}_{LS2}Fe^{II}_{LS2})Fe^{III}_{LS}]$ state. At low temperature, a photo-induced state at 808 nm at 5 K is formed and shows (i) ferromagnetic interactions between the photogenerated Co(II)

and Fe(III) centers, and (ii) relaxes to the thermodynamic [$Fe^{III}_{LS}(Co^{III}_{LS2}Fe^{II}_{LS2})Fe^{III}_{LS}$] state at 130 K. Interestingly, the photoinduced state shows a frequency dependence of the χ' and χ'' susceptibilities below 4 K. This behavior, characteristic of single molecule magnets, was triggered by light and gives rise for the first time to a magnetic bistability in a molecular object. This situation is similar to photomagnet behavior, although no magnetic phase transition is present.

Photo-induced magnetic bistability has been also reported in extended systems. For instance, 1D chains have been structurally characterized in **15**[46] and **22**[68] and both display thermally- and photo-induced ET. Due to their extended structures, magnetic correlation length between photo-induced paramagnetic Co^{II} and Fe^{III} ions generate Single-Chain Magnet behaviors (SCM), the analoguous magnetic phenomenon as SMM in 1D chains. These photo-induced SMM and SCM properties remain very rare in the literature, found in SCO systems,[69,70,71] or in ET Fe/Co compounds.[47,68,72] They are very interesting for data storage devices because they present three different states addressed by the judicious use of light and a magnetic field. The term of tristabililty has been used to describe similar phenomena, ie. photoinduced SMM in SCO compounds.

The same year, a linear trinuclear molecule [Co_2Fe] **23** was published by Sato group.[73] **23** exhibits thermal and photo-induced ET that imposes a change from a centro-symmetric non polar [$Fe^{III}_{LS}Co^{II}_{HS}Fe^{III}_{LS}$] state into a symmetric [$Fe^{III}_{LS}Co^{III}_{LS}Fe^{II}_{LS}$] polar one. This result shows for the first time the possibility of triggering a polarity switch by an ET process. This result suggests that an electric field can be used to direct the ET in molecular materials. For instance some calculations predict electric-field control of ET in FeCo pairs.[74] This research direction merits to be further investigated in the future.

Conclusion

Since the discovery of the photomagnetic effect in Fe/Co Prussian blue analogs in 1996, an intense research has been devoted to the synthesis and characterization of new Fe/Co cyanido-bridged molecules. Today, a large family of coordination compounds has been reported and their structural and electronic properties show strong similarities with spin crossover compounds. The Fe/Co systems are well described with two states: one made of diamagnetic $Fe^{II}Co^{III}$ units and the second one made of paramagnetic $Fe^{II}Co^{III}$ units. Thermally-induced metal-to-metal electron transfer is often observed in 165-300 K range between the high-temperature paramagnetic state to the low-temperature diamagnetic state and can be gradual or abrupt depending of the presence of intermolecular interactions between the molecules. Electron transfer has been studied in solid state and in solutions. The solution media offer the possibility to tune the thermally-induced electron transfer temperature for each system with electronic effects on the ligands around the metal centers. At low temperature, light-induced electron transfer is observed and corresponds to the population of the paramagnetic state. This photo-induced state is persistent towards 180 K, which is a record for coordination compounds. Moreover, the control of the thermal stability of the light-induced ET depends on the polynuclearity of the systems, being lower for a [FeCo] pair and becoming higher for the [Fe_4Co_4] cube. The present and future developments of these systems concern the exploration of other metal ions couples, for instance W/Co or Co/Os, and/or the addition of another properties like dielectric properties or chirality in order to create synergy between the electron transfer and another property. This route towards multifunctional systems is very attractive and challenging. Moreover, the synthesis and characterization of small switchable electron transfer compounds is an important step for both fundamental and applied researches. Actually the pairs and squares are ideal models to develop sophisticated physical measurements using time resolved techniques in solutions and in solid state, but also theoretical predictions. The development of applications using these smart molecules seems easier compared to their 3D analogs because their solubility will facilitate their integration in devices.

Acknowledgements

The author wish to thank all past and actual collaborators, at the Institut de Chimie de la Matière Condensée et du Centre de Recherche Paul Pascal and abroad, and particularly Dr. Rodolphe Clérac for his active participation to the project of Fe/Co compounds in Bordeaux and Elizabeth Hillard for her help in the final form of this manuscript. The author is grateful to the University of Bordeaux, the CNRS and the Région Aquitaine for funding.

Keywords: electron transfer • molecular magnetism • photomagnetism • cyano-metallates • spin crossover

[1] R. Willet, D. Gatteschi, O. Kahn, *Magneto-Structural Correlations in Exchange coupled Systems* **1985**, *Vol C40*, Reidel.

[2] *Introduction to Molecular Magnetism*, Eds.: C. Benelli, D. Gatteschi, Wiley-VCH, Weinheim, **2015**, pp. 1-23.

[3] a) O. Kahn, J. Krober, C. Jay, *Adv. Mater.* **1992**, *4*, 718. b) O. Kahn, C. Jay Martinez, *Science* **1998**, *279*, 44.

[4] a) S. Decurtins, P. Gütlich, C. P. Kohler, H. Spiering, A. Hauser, *Chem. Phys. Lett.* **1984**, *105*, 1. b) S. Decurtins. P. Giitlich, K. M. Hasselbach, A. Hauser, H. Spiering, *Inorg. Chem*. **1985**, *24*, 2174.

[5] A. Hauser, *J. Chem. Phys*. **1991**, *94,* 2741.

[6] P. Gütlich, H. A. Goodwin, Topics in Current Chemistry *Spin crossover in transition metal compounds* **2004** *Vol 233-235* Springer Verlag Berlin Heidelberg.

[7] M. A. Halcrow, *Spin crossover materials : properties and applications* **2013** John Wiley & Sons, Ltd, Oxford, UK.

[8] O. Sato, *Nat. Chem.* **2016**, *8,* 644.

[9] T. Tezgerevska, K. G. Alley, C. Boskovic, *Coord. Chem. Rev.* **2014***, 268*, 23.

[10] A. Bleuzen, V. Marvaud, C. Mathonière, B. Sielklucka, M. Verdaguer, *Inorg. Chem*. **2009,** *48*, 3453.

[11] K. Dunbar, C. Achim, M. Shatruk, chapter 6, **2013** in ref [7].

[12] D. Aguila, Y. Pardo, E. Koumousi, C. Mathonière, R. Clérac, *Chem. Soc. Rev.* **2016**, *45*, 203.

[13] B. Sieklucka, D. Pinkowicz, *Molecular magnetic materials: Concepts and Applications,* Wiley-VCH, Verlag GmbH & Co, KGaA, 2017

[14] O. Sato, T. Iyoda, A. Fujishima, K. Hashimoto, *Science* **1996**, *272*, 704.

[15] a) O. Sato, Y. Einaga, T. Iyoda, A. Fujishima, K. Hashimoto, *Inorg. Chem.* **1999**, *38*, 4405; b) A. Bleuzen, C. Lomenech, V. Escax, F. Villain, F. Varret, C. Cartier dit Moulin, M. Verdaguer, *J. Am. Chem. Soc.* **2000**, *122*, 6648; c) V.

Escax, A. Bleuzen, C. Cartier dit Moulin, F. Villain, A. Goujon, F. Varret, M. Verdaguer, *J. Am. Chem. Soc.* **2001**, *123*, 12536; d) N. Shimamoto, S.-i. Ohkoshi, O. Sato, K. Hashimoto, *Inorg. Chem.* **2002**, *41*, 678.
[16] a) C. Cartier dit Moulin, F. Villain, A. Bleuzen, M.-A. Arrio, P. Sainctavit, C. Lomenech, V. Escax, F. Baudelet, E. Dartyge, J.-J. Gallet, M. Verdaguer, *J. Am. Chem. Soc.* **2000**, *122*, 6653; b) G. Champion, V. Escax, C. Cartier dit Moulin, A. Bleuzen, F. Villain, F. Baudelet, E. Dartyge, M. Verdaguer, *J. Am. Chem. Soc.* **2001**, *123*, 12544.
[17] D. Li, R. Clérac, O. Roubeau, E. Harté, C. Mathonière, R. Le Bris, S. M. Holmes, *J. Am. Chem. Soc.* **2008***, 130,* 252-257.
[18] a) Y. Zhang, D. Li, R. Clérac, M. Kalisz, C. Mathonière, S. Holmes, *Angew. Chem. Int. Ed.* **2010**, *49*, 3752. b) M. Nihei, Y. Sekine, N. Suganami, H. Oshio, *Chem. Lett.* **2010**, 39, 978; c) M. Nihei, Y. Sekine, N. Suganami, K. Nakasawa, H. Nakao, Y. Murakawi, H. Oshio, *J. Am. Chem.* Soc. **2011**, *133*, 3592; d) J. Mercurol, Y. Li, E. Pardo, O. Risset, M. Seuleiman, H. Rousselière, R. Lescouezec, M. Julve, *Chem. Comm.* **2010**, *46*, 8995.
[19] E.S. Koumousi, I.-R. Jeon, Q. Gao, P. Dechambenoit, D. N. Woodruff, P. Merzeau, L. Buisson, X. Jia, D. Li, F. Volatron, C. Mathonière, R. Clérac, *J. Am. Chem. Soc.* **2014**, *136*, 15461.
[20] D. Siretanu, D. Li, L. Buisson, D. M. Bassani, S. M. Holmes, C. Mathonière, R. Clérac, *Chem. Eur. J.* **2011,** *17*, 11704.
[21] R. Boca, *Theoretical Foundations of Molecular magnetism* **1999**, *Vol. 1*, Elsevier, Netherlands.
[22] a) Kahn, O. *Molecular Magnetism*; VCH: New York, **1993**. b) A. Koudriavtsev, R. F. Jameson, W. Linert, *The Law of Mass Action*, Springer-Verlag Berlin Heidelberg **2001**.
[23] E. König, *Struct. Bond.* **1991**, *76*, 51.
[24] M. Nihei, Y. Yanai, Y. Sekine, H. Oshio, *Angew. Chem. Int. Ed.*, **2017**, *56*, 591.
[25] Y. Sekine, M. Nihei, H. Oshio, *Chem. Eur. J.*, **2017**, *23*, 5193
[26] L. Cambi, L. Szebo, *Chem Ber. Dtsch. Ges.* **1931** 2591.
[27] J. -F. Létard, J. Mater. Chem., **2006**, *16*, 2550.
[28] V. Escax, A. Bleuzen, C. Cartier dit Moulin, F. Villain, A. Goujon, F. Varret, M. Verdaguer, *J. Am. Chem. Soc.* **2001**,*123*, 12536.
[29] R. Herber, L. M. Casson, *Inorg. Chem.* **1986**, *25*, 847. b) J.-F. Létard, *Mater. Chem.*, **2006**, *16*, 2550.
[30] a) J. S. Costa, C. Balde, C. Carbonera, D. Denux, A. Wattiaux, C. Desplanches, J.-P. Ader, P. Gütlich, J.-F. Létard, *Inorg. Chem.* **2007**, *46*, 4114. b) S. Hayami, Z.-z. Gu, Y. Einaga, Y. Kobayashi, Y. Ishikawa, Y. Yamada, A. Fujishima, O. Sato, *Inorg. Chem.* **2001**, *40*, 3240. c) P. Guionneau, F. Le Gac, A. Kaiba, J. S. Costa, D. Chasseau, J. -F. Létard, *Chem Comm.* **2007**, 3723.
[31] S. Gawali-Salunke, F. Varret, I. Maurin, C. Enachescu, M. Malarova, K. Boukheddaden, E. Codjoiv, H. Tokoro, S.-i. Okhoshi, K. Hashimoto, *J. Phys. Chem. B* **2005**, *109*, 8251.
[32] V. Gomez, C. Saenz de Pipaon, P. Maldonado-Illescas, J. C. Waerenborgh, E. Martin, J. Benet-Buchholz, J. Ramon Galan-Mascaros, *J. Am. Chem. Soc.* **2015**, *137*, 11924.
[33] D. Garnier, J.-R. Gimenez, Y. Li, J. von Bardeleben, Y. Journaux, T. Augenstein, E. M. B. Moos, M. T. Gamer, F. Breher, R. Lescouezec, *Chem. Sci.* **2016**, *8*, 4763.
[34] Y. Sekine, M. Nihei, R. Kumai, H. Nakao, Y. Murakami, H. Oshio, *Chem. Comm.* **2014**, *50,* 4050.
[35] A. Mondal, Y. Li, M. Seuleiman, M. Julve, L. Toupet, M. Buron-Le Cointe, R. Lescouëzec, *J. Am. Chem. Soc*. **2015**, *135*,1653.
[36] Y. Sekine, M. Nihei, R. Kumai, H. Nakao, Y. Murakami, H. Oshio, *Inorg. Chem. Front.* **2014**, *1*, 540.
[37] B. P. Macpherson, P. V. Bernhardt, A. Hauser, S. Pages, E. Vauthey, *Inorg. Chem.* **2005**, *44,* 5530.
[38] Y. Moritomo, F. Nakada, H. Kamioka, T. Hozumi, S.-i. Ohkoshi, *Phys. Rev. B* **2007**, *75*, 214110.
[39] a) C. P. Berlinguette, A. Dragulescu-Andrasi, A. Sieber, J. R. Galán-Mascarós, H. U. Güdel, C. Achim, K. R. Dunbar, *J. Am. Chem. Soc.* **2004**, *126*, 6222; b) C. P. Berlinguette, A. Dragulescu-Andrasi, A. Sieber, H. U. Güdel, C. Achim, K. R. Dunbar, *J. Am. Chem. Soc.* **2005**, *127*, 6766; c) M. Shatruk, A. Dragulescu-Andrasi, K. E. Chambers, S. A. Sto- ian, E. L. Bominaar, C. Achim, K. R. Dunbar, *J. Am. Chem. Soc.* **2007**, *129*, 6104.
[40] G. N. Newton, M. Nihei, H. Oshio, *Eur. J. Inorg. Chem*. **2011**, 3031.
[41] S. Zerdane, M. Cammarata, L. Balducci, R. Bertoni, L. Catala, S. Mazerat, T. Mallah, M. N. Pedersen, M. Wuff, K. Nakagawa, H. Tokoro, S.-i. Ohkoshi, E. Collet, *Eur.J. Inorg. Chem.* **2017**, DOI: 10.1002/ejic.201700657
[42] W. D. Griebler, D.Z. Babel Naturforsch. B **1982**, 37,832.
[43] S. Ferlay, T. Mallah, R. Ouhaes, P. Veillet, M. Verdaguer, Nature **1995**, *78*, 701.
[44] O. Sato, Y. Einaga, A. Fujishima, K. Hashimoto, *Inorg. Chem.* **1999***, 38*, 4405.
[45] G. Champion, V. Escax, C. Cartier dit Moulin, A. Bleuzen, F. Villain, F. Baudelet, E. Dartyge, M .Verdaguer, *J. Am. Chem; Soc.*, **2001**, *123*, 12544.
[46] N. Hoshino, F. Iijima, G. N. Newton, N. Yoshida, T. Shiga, H. Nojiri, A. Nakao, R. Kumai, Y. Murakami, H. Oshio, *Nat. Chem.* **2012**, *4*, 921.
[47] M. Nihei, Y. Okamoto, Y. Sekine, N. Hoshino, T. Shiga, I. Po-Chun Liu, H. Oshio, *Angew. Chem. Int. Ed.* **2012**, *124,* 1.
[48] E. Pardo, M. Verdaguer, P. Herson, H. Rousseliere, J. Cano, M. Julve, F. Lloret, R. Lescouezec, *Inorg. Chem.* **2011**, *50*, 6250.
[49] R. A. Marcus, *Chem. Phys. Lett.* **1987**, *133*, 471.
[50] Y.-Z. Zhang, P. Ferko, D. Siretanu, R. Ababei, N. P. Rath, M. J. Shaw, R. Clérac, C. Mathonière, S. M. Holmes, *J. Am. Chem. Soc,* **2014***, 136*, 16854.
[51] I.-R. Jeon, S. Calancea, A. Panja, D. M. Pinero Cruz, E. S. Koumousi, P. Dechambenoit, C. Coulon, A. Wattiaux, P. Rosa, C. Mathonière, R. Clérac, *Chem. Science* **2013**, *4*, 2453.
[52] Y. Sekine, M. Nihei, H. Oshio, *Chem Lett.* **, 2014***, 43,* 1029.
[53] R.-J. Wei, T. Shiga, G.N. Newton, D. Robinson, S. Takeda, H. Oshio, *Inorg. Chem.* **2016**, *55,* 12114.
[54] S.-i. Ohkoshi, H. Tokoro *Acc. Chem. Res.* **2012**, *45* 174.
[55] a) H. Tokoro, S.-i. Ohkoshi, T. Matsuda, K. Hashimoto, *Inorg. Chem.* **2004**, *55*, 5231. b) H. Tokoro, T. Matsuda, T. Nuida, Y. Moritomo, K. Ohoyama, E. D. Loutete Dangui, K. Boukheddaden, S.-i Ohkoshi *Chem. Mater*. **2008**, *20*, 423.
[56] S.-i. Ohkoshi, Y. Einaga, A. Fujishima, K. Hashimoto *J. Electro-Anal. Chem.* **1999**, *473*, 245.
[57] C. Avendano, M. G. Hilfiger, A. Prosvirin, C. Sanders, D. Stepien, K. R. Dunbar, *J. Am. Chem. Soc*. **2010**, *132*, 13123.
[58] Y. Arimoto, S. Ohkoshi, Z. J. Zhong, H. Seino, Y. Mizobe, K. Hashimoto, J*. Am. Chem. Soc*. **2003**, 125, 9240.
[59] S. Ohkoshi, S. Ikeda, T. Hozumi, T. Kashiwagi, K. Hashimoto, *J. Am. Chem. Soc.*, **2006**, *128*, 5320.
[60] A. Mondal, L.-M. Chamoreau, Y. Li, Y. Journaux, M. Seuleiman, R. Lescouezec, *Chem. Eur. J.* **2013**, *24*, 7682.
[61] R. Podgajny, S. Chorazy, W. Nitek, M. Rams, A. M. Majcher, B. Mrzalek, J. Zukrowski, C. Kapusta, B. Sieklucka, *Angew. Chem. Int. Ed.* **2012**, *52*, 896.
[62] M. G. Hilfiger, M. Chen, T. V. Brinzari, T. M. Nocera, M. Shatruk, D. T. Petasis, J. L. Musfeldt, C. Achim, K. R. Dunbar, *Angew. Chem. Ind. Ed.*, **2010**, *49*, 1410.
[63] a) S.-i. Ohkoshi, H. Tokoro, T. Hozumi, Y. Zhang, K. Hashimoto, C. Mathonière, I. Bord, G. Rombaut, M. Verelst, C. C. D. Moulin, F. Villain, *J. Am. Chem. Soc.* **2006**, *128*, 270. b) T. Hozumi, K. Hashimoto, S. Ohkoshi, *J. Am. Chem. Soc.* **2005**, *127*, 3864. c) F. Volatron, D. Heurtaux, L. Catala, C. Mathonière, A. Gloter, O. Stéphan, D. Repetto, M. Clemente-León, E. Coronado, T. Mallah, *Chem. Commun*. **2011**, *47*, 1985.
[64] J. M. Herrera, V. Marvaud, M. Verdaguer, J. Marrot, M. Kalisz, C. Mathonière, *Angew. Chem. Int. Ed.* **2004**, *43*, 5468.
[65] a) M. -A. Arrio, J. Long, C. Cartier dit Moulin, A. Bachschmitt, V. Marvaud, A., Rogalev, C. Mathonière, F. Wilhem, P. Sainctavit, **2010**, *J. Phys. Chem. C, 114*, 593. b) S. Brossard, F. Volatron, L. Lisnard, M.-A. Arrio, L. Catala, C. Mathonière, T. Mallah, C. Cartier dit Moulin, A. Rogalev, F. Wilhelm, A. Smekhova, P. Sainctavit, *J. Am. Chem. Soc.,* **2012**, *134*, 222. c) M.-A. Carvajal, M. Reguero, C. de Graaf, *Chem. Commun.*, **2010**, *46*, 5737. d) M. A. Carvajal, R. Caballol, C. de Graaf, *Dalton Trans.*, **2011**, *40*, 7295. e) N. Bridonneau, J. Long, J.-L. Cantin, J. von Bardeleben, S. Pillet, E.-E. Bendeif, D. Aravena, E. Ruiz, V. Marvaud, **2015**, *Chem. Commun*., *51*, 8229.
[66] a) G. Rombaut, M. Verelst, S. Golhen, L. Ouahab, C. Mathonière, O. Kahn, O., *Inorg. Chem.* **2001**, *40*, 1151; a) C.Mathonière; H. Kobayachi, R. Le Bris, A. Kaiba, I. Bord, 2008 *C. R. Chimie* **2008**, *11*, 665. c) W. Zhang, H.-L. Sun, O. Sato, *Dalton Trans.* **2011**, *40*, 2735. d) H. Xu, O. Sato, Z. Li, J., Ma., *Inorg. Chem. Commun.*, **2012**, *15*, 311. e) C. Maxim, C. Mathonière, M. Andruh, *Dalton Trans.* **2009**, 7805. f) O. Stefanczyk, A. M. Majcher, M. Rams, W. Nitek, C. Mathonière, B. Sieklucka, *J. Mater. Chem. C* **2015**, *3*, 8712. j) W. Zhang, H.-L. Sun, O. Sato, O. *CrystEngComm.*, **2010**, 12, 4045. h) T. Korzeniak, D. Pinkowicz, W. Nitek, T. Danko, R. Pelka, B. Sieklucka, *Dalton Trans.*, **2016**, *45*, 16585.
[67] R. Sessoli, D. Gatteschi, J. Villain, Molecular Nanomagnets in *Mesoscopic Physics and Nanotechnology* **2006**, Oxford, Great Britain.
[68] D. P. Dong, T. Liu, S. Kanegawa, S. Kang, O. Sato, C. He, C.-Y. Duan, *Angew. Chem., Int. Ed.*, **2012**, *51*, 5119.
[69] X. Feng, C. Mathonière, I.-R. Jeon, M. Rouzières, A. Ozarowski, M. L Aubrey, M. I. Gonzales, R. Clérac, J. R. Long, *J. Am. Chem. Soc.* **2013**, *135*, 15880.
[70] C. Mathonière, H.-J. Lin, D. Siretanu, R. Clérac, J. M. Smith, *J. Am. Chem. Soc.* **2013**, *135*, 19083.
[71] T. Liu, H. Zheng, S. Kang, Y. Shiota, S. Hayami, M. Mito, O. Sato, K. Yoshizawa, S. Kanegawa, C. Duan, *Nat. Comm.* **2013**, 10.1038/ncomms3826.
[72] T. Liu, Y.-J. Zhang, S. Kanegawa and O. Sato, *J. Am. Chem. Soc.* **2010**, *132*, 8250.
[73] T. Liu, D.-P. Dong, S. Kanegawa, S. Kang, O. Sato, Y. Shiota, K. Yoshizawa, S. Hayami, S. Wu, C. He, C.-Y. Duan. *Angew. Chem. Int. Ed.* **2012**, *51*, 4367
[74] M. Roman, S. Descurtins, S.-X. Liu, S. Klokishner, *Eur. Jour. Inorg. Chem.* **2016**, 5324.

Entry for the Table of Contents (Please choose one layout)

MICROREVIEW

Switchable coordination compounds have known a rapid development in the last 30 years since they can show bistability at the molecular scale. Here, we focus on a family of compounds imagined by chemists to create molecular fragments of the 3D Prussian blue analogs. The remarkable properties of these cyanido-bridged Fe-Co molecules, in particular the thermally-induced and light-induced electron transfer are presented.

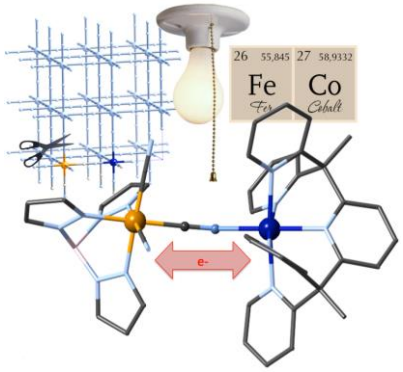

Switching molecules*

*Corine Mathonière**

Page No. – Page No.

Metal-to-Metal Electron Transfer: a powerful tool for the design of new switchable compounds

* electron transfer and switching properties in Prussian blue molecular analogs